ENGINEERING TRANSACTIONS • *Engng. Trans.* • **50**, 4, 323–357, 2002
Polish Academy of Sciences • Institute of Fundamental Technological Research

MODELLING AND SIMULATION OF FILTRATION IN THE DEVELOPMENT OF WATER TREATMENT TECHNOLOGIES

K. WOJCIECHOWSKA

Silesian University of Technology,
Institute of Water and Wastewater Engineering,
18 Konarskiego Str.,
44-100 Gliwice

The paper presents modelling and simulation of water filtration in a multilayer rapid filter. As far as modelling is concerned, a combination of phenomenological and theoretical models was described. Special attention is paid to modelling of the filter coefficient. The model developed is a basis for filtration simulation in the filter bed. Simulation results for the concentration of particles in the filtered water, concentration of particles deposited in the bed and the headloss in the bed are presented as 3D diagrams. They are consistent in quality with the values obtained in the physical process which is discussed in the analysis herein. Thus, it can be concluded that the model for the process was selected correctly, its parameters were set appropriately and the numerical solution of partial differential equations involved in the model was also correct. The developed numerical model may serve as a new tool for development of water treatment technologies. Numerical simulations were carried out, applying the "Mathematica" program.

1. INTRODUCTION

Water filtration in a multilayer rapid filter is a complex physico-chemical process that constitutes one of the basic elements in water treatment technology. Modelling of the process consists in distinction of the types of occurring phenomena and selection of a level (microscopic, macroscopic) at which they are described, next selection of variables that are of interest due to an objective of the process, assignment of quantitative measures to all variables, and finally determination of quantitative relations between the variables. By 1970, most researches employed the phenomenological approach. If one applies this approach and the simplest form of the model, then filtration is described by two equations (IWASAKI, 1937) [13]. The first describes removal of particles and filter coefficient is its basic parameter. The other describes the mass balance. Later on the investigations concentrated on finding a dependence of the filter coefficient on

its initial value as for the clean bed, and the process conditions, such as size of the particles, filtration velocity and others. The correlation between the filter coefficient and concentration of particles deposited in the bed was of a special interest to researchers. Dealing with this problem an approach, initiated by STEIN as early as 1940, based on analysis of particle trajectory (YAO *et al.*, 1971) [32], (TIEN *et al.*, 1979) [23, 24], has been developed since 1970. The trajectory analysis involves a simplified model of the flow around the grain and calculates the trajectories that the particles follow, making it possible to determine the probability of particles retention by the bed grain. Forces that affect the probability of particle retention and, consequently, the efficiency of particle removal were determined. Filtration modelling was undertaken by many investigators. O'MELIA and ALI (1978) [20] and O'MELIA and STUMM [19] contributed significantly to the development of filtration modelling by stating that particles act as collectors and are responsible for an increase in the efficiency of particle retention, what resulted in an increase in filter coefficient during the initial phase of filtration resulted from. CHANG and TIEN, (1985) [7], proposed a dendrite model for the explanation of increase in the efficiency of particles removal caused by presence of the particles deposited earlier. In this model, complexity of the dendrite tree increases with the number of particles deposited and, in turn, modelling becomes more difficult. TIEN suggested a way to overcome the problem, which renders particle deposition impossible by blocking the pores what means the same as elimination of branches of the dendrite tree. In the works of TIEN *et al.*, (1979) [23, 24], and CHOO and TIEN (1975) [8], it was assumed that the deposited particles are porous themselves, while most of the earlier works assumed that a layer of particles is not of porous nature. In this paper, it has been found that the porous structure of the particle deposit enables the fluid to flow through their pores and increases the efficiency of particle removal. Further progress in the study of filtration was made when it was found that particle size distribution (PSD) plays an important role in filtration. Most of the earlier investigations treated suspension as a set of particles suspended in water, applying an average particle size to the description of its characteristics. The works of DARBY and LAWLER (1990) [9], TOBIASSON *et al.* (1990) [27], VIGNESWARAN *et al.*, (1990) [28], MACKIE and BAI (1993) [14] showed that particle size distribution is more important than it was believed to be. MACKIE and BAI (1993) [14] emphasized that particles of different size are removed selectively, thus PSD changes both in time and through the bed depth. STEVENSON (1997) [22] investigated the influence of the grain size distribution of the filtered medium on quality of the filter performance. The discussed results on filtration models, initiated by IVES and extended by CAMP [3], CLEASBY [4, 5, 6], MINC [16], MOHANKA [17, 18], O'Melia [20], RAJAGOPALAN [21], STEVENSON [22], TIEN [23, 25, 26], ADINIDA and REBHUN [1] and the development of methods and software, enable numerical

simulation of filtration. Consistency between the variables obtained as a result of simulation and the values observed in the physical process is a measure of model quality and correctness of the simulation process. This consistency enables to replace the physical process with the numerical simulation as far as design operation and control [29, 30] of rapid filters are concerned. The number of papers dealing with numerical simulation of filtration is not large [2, 15], and the information included becomes out of date very fast due to the development of software for numerical integration of partial differential equations. Paper [2] may serve as an example. It proposes procedure D03PEF from NAG library in Fortran for an integration of a system of partial equations. In this paper, the filtration model is divided into three fragments: mass balance, filtration kinetics and headloss. The chapter named Numerical Solution of filtration equations deals with digitisation used for numerical integration of the model equations. The latter part of the chapter points to the problem of identification of model parameters and presents a solution to the problem, suggesting a discrete version of the model. Subsequent chapters contain simulation results with commentary on their qualitative consistency with the findings obtained from a real filtration process.

2. Filtration modelling

The rate equation for the deposit mass balance links the rate of change in particle concentration in the filtered water with the rate of change in concentration of particles accumulated in the bed. It means that measurements of a change in particle concentration in the filtered water for a given bed depth can serve as a basis for evaluation of the change in the concentration of particles accumulated in the bed at the same depth. Particles concentration in the filtered water is expressed as mass per unit volume and is called absolute specific deposit, while for the concentration of particles accumulated in the bed, the choice of units is based on additional conditions. It is very convenient to formulate the deposit balance, applying mass units; however, in the kinetic and headloss equations the bulk specific deposit $\frac{v}{v}$ rather than absolute specific deposit $\frac{m}{v}$ is required. It results from the fact that kinetics and headloss are caused by bed porosity which depends on bulk specific deposit $\frac{v}{v}$. Two approaches are possible. In the first one the balance equation is formulated for the absolute specific deposit which is subsequently converted into bulk specific deposit in a separate equation, and in the other the balance equation is formulated for the bulk specific deposit which makes the equation more complex. Thus, the determination of the bulk specific deposit accumulated in the bed is an integral part of filtration modelling. If the porosity of the material deposited equals 0, it is easy to convert the bulk

specific deposit into the absolute specific deposit. But in fact, the conversion of the absolute specific deposit into the bulk specific deposit (or inversely) is not that easy since the density of the porous material deposited must be known. The density changes in the curse of filtration are largely dependent upon the process parameters. The conversion of the absolute specific deposit into the bulk specific deposit is performed as follows: the product of so-called bulk coefficient and absolute specific deposit yields an evaluation of the bulk specific deposit. In the simplest case, the bulk coefficient is regarded as constant. In more complex approaches, the bulk coefficient is assumed as variable with the absolute specific deposit. MOHANKA (1969) [17] summarized the existing experimental methods which enable determination of the bulk specific deposit, including the possibility for estimation of the bulk specific deposit based on the headloss model. In this paper, the following equation was applied to convert the absolute specific deposit into the bulk specific deposit:

$$\sigma_0(t, L) = \frac{\sigma(t, L)}{\rho_s c_3 c_4 (v(t))} \tag{2.1}$$

in which $\sigma(t, L)[\mathrm{g/m^3}]$ is the absolute specific deposit in the bed at time t, at depth L, $\sigma_0(t, L)$ is the bulk specific deposit and $\rho_s[\mathrm{g/m^3}]$ is arbitrary density of the deposited material. The assumed dependence includes the influence of filtration velocity on the relation between the bulk and absolute specific deposits. Since the assumed dependence contains a product of coefficients c_3, c_4, one of them was adjusted arbitrarily to 0.2 [1/m] and c_3 was chosen as a result of numerical trials. The range considered was $1.2\ 10^{-3} - 6.3\ 10^{-3}$. The selected numerical values of coefficients has no physical proof. In the case of constant velocity in the bed cross-section and one-dimensional flow, the mass balance equation can be obtained by examining an elementary fragment of the bed selected at a depth of L and in time t, see Fig.1.

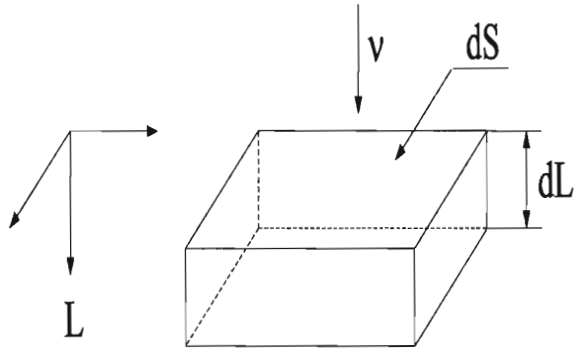

FIG. 1. An elementary fragment of the bed selected at a depth of L at time t.

The mass of particles inflowing in filtered water to the elementary bed volume is $v(t)C(t,L)dSdt$ while the outflowing mass is $v(t)C(t,L)dSdt + \frac{\partial}{\partial L}(v(t)C(t,L))$ $dSdt$, thus the change of the mass occurring in the elementary bed volume is equal to $v(t)\frac{\partial}{\partial L}C(t,L)dSdtdL$.

Due to the continuity law that states that the mass of particles removed from the flowing suspension is equal to the mass of particles accumulated on bed grains or in filtered water filling bed pores, we receive the following mass balance equation for the elementary volume:

$$(2.2)\quad v(t)\frac{\partial}{\partial L}C(t,L)\ dS\ dt\ dL + \frac{\partial}{\partial t}\sigma(t,L)\ dS\ dt\ dL + (\varepsilon_0 - \sigma_0(t,L))\frac{\partial}{\partial t}C(t,L)dS\ dt\ dL = 0,$$

where $C(t,L)$ [g/m^3] is concentration of particles in filtered water, $\sigma(t,L)$ [g/m^3] is the absolute specific deposit, both in time t[h] and at a depth of L[m], $v(t)$[m/h] is filtration velocity which does not depend on L, ε_0 is the initial bed porosity and $\varepsilon_0 - \sigma_0(t,L)$ is porosity at time t and at a depth L resulting from the bulk specific deposit.

Finally the mass balans equation has the form:

$$(2.3)\quad v(t)\frac{\partial}{\partial L}C(t,L) + \frac{\partial}{\partial t}\sigma(t,L) + (\varepsilon_0 - \sigma_0(t,L))\frac{\partial}{\partial t}C(t,L) = 0.$$

Taking into account diffusion of particles suspended in the filtered water, the most general form of Eq. (2.3) is:

$$(2.4)\quad v(t)\frac{\partial}{\partial L}C(t,L) + \frac{\partial}{\partial t}\sigma(t,L) + (\varepsilon_0 - \sigma_0(t,L))\frac{\partial}{\partial t}C(t,L) = D\ \frac{\partial^2}{\partial L^2}C(t,L),$$

where D[m^3/s] denotes one-dimensional diffusion coefficient for particles suspended in the filtered water.

The assumption $(\varepsilon_0 - \sigma_0(t,L))\frac{\partial}{\partial t}C(t,L) = 0$ and $D = 0$ yields the simplest and most frequently assumed form of the mass balance equation (continuity equation), see eg. works of Minc [16] and Ives [11] as well as more recent works like Mackie [14].

$$(2.5)\quad \frac{\partial}{\partial t}\sigma(t,L) + v\frac{\partial}{\partial L}C(t,L) = 0.$$

The kinetics of filtration may be described in many ways. The historically oldest and notationally simplest approach describes the kinetics of particles removal from filtered water flowing through the bed, applying the notion of filter

coefficient which determines "the efficiency of particles removal". In the literature, [12, 11, 23, 17], [31], models of kinetics were formulated in various forms, sometimes different from that proposed in this paper. In one of the forms, a kinetic equation states that a change in concentration of particles in filtered water per bed depth unit is proportional to this concentration. The equation in the form proposed by IWASAKI [13] is as follows:

$$\frac{\partial C(t,L)}{\partial L} = -\lambda C(t,L) \tag{2.6}$$

where $\lambda[\mathrm{m}^{-1}]$ is the filter coefficient. The filter coefficient is a measure of filter performance and is dependent on parameters, such as type and size of bed grain, filtration velocity, physico-chemical properties of filtered water and concentration of particles deposited in the bed. A model function:

$$\lambda = f(\lambda_0, \sigma(t,L), v(t)) \tag{2.7}$$

describing the filter coefficient by means of its initial value, bulk specific deposit and filtration velocity proposed by Ives is the most popular:

$$\lambda(\sigma(t,L), v(t) = \lambda_0(v(t)) \left(1+\beta\frac{\sigma_0(t,L)}{\varepsilon_0}\right)^x \left(1-\frac{\sigma_0(t,L)}{\varepsilon_0}\right)^y \left(1-\frac{\sigma(t,L)}{\sigma_u(v(t))}\right)^{z(v(t))} \tag{2.8}$$

where

$$\lambda_0(v(t)) = C_1 \frac{S^{1.35}}{v(t)^{0.25}}, \tag{2.9}$$

$$S = \frac{6(1-\varepsilon_0)}{\psi d_s}, \tag{2.10}$$

$$\beta = \frac{a}{S^{0.65}}, \tag{2.11}$$

$$z(v) = c_2 \frac{S^{0.61}}{v(t)^{0.24}}, \tag{2.12}$$

where σ_u $[\mathrm{g/m}^3]$ is a concentration of particles for which the filter coefficient equals zero. This model includes three types of influence on the filter coefficient, and additionally, its value depends on exponents x, y, z determined experimentally. The first factor in the brackets takes into consideration an increase in the

specific bed surface resulting from deposition on the bed grain. The second one takes into account a decrease in bed porosity during a filtration run in relation to its initial porosity resulting from deposition in the pores. The third takes into consideration an increase in average filtration velocity resulting from a reduction in cross-section of the pores brought about by deposits. As the simulations carried out have shown, this dependence is qualitatively typical. However, higher concentrations of particles accumulated in the bed and variable filtration velocity require a more accurate model. This dependence does not describe precisely the initial phase of filtration in which the filter coefficient increases due to improved retention (ripening of the filter) caused by the particles deposited on the gains. During filtration, as its front moves deeper into the bed, the porosity distribution changes as the function of the bed depth due to the deposition of the particles, thus the filter coefficient also changes with depth L and filtration time t. The issue concerning determination of concentration of particles deposited in the bed and in filtered water with respect to time and depth in multilayer filters was presented by MOHANKA [17, 18]. In the literature dealing with filtration, the additivity of a loss at a flow through the clean bed and the loss resulting from accumulation of particles in the bed is very common. Specific losses at the flow through the clean bed are expressed by the equation [17, 18]:

$$\frac{\partial}{\partial L}h_0(t,L) = \frac{K_0\mu v(1-\varepsilon_0)^2}{\rho g \varepsilon_0^3 \psi^2 d_s^2}, \tag{2.13}$$

where K_0 is the Kozena constant. Additional specific losses resulting from particle accumulation may be expressed by [4, 6]:

$$\frac{\partial}{\partial L}h_a(t,L) = b_1\left(\frac{6(1-\varepsilon_0)}{\psi d_s}\right)^{0.9} v^{0.4}\sigma(t,L), \tag{2.14}$$

where $h_a(t,L)$[m] represents additional head losses and $\sigma(t,L)$[g/m^3] is concentration of particles accumulated on the depth of L, in time t[h].

Respectively to (2.13), (2.14):

$$\frac{\partial}{\partial L}h(t,L) = \frac{K_0\mu v(1-\varepsilon_0)^2}{\rho g \varepsilon_0^3 \psi^2 d_s^2} + b_1\left(\frac{6(1-\varepsilon_0)}{\psi d_s}\right)^{0.9} v^{0.4}\sigma(t,L). \tag{2.15}$$

Depending upon the selected co-ordinate system (direction of axis L) and taking into account a water layer over the bed, a pressure line equation (resulting from an equation for headloss in the bed) is as follows:

$$\frac{\partial}{\partial L}h(t,L) = 1 - \frac{K_0\mu v(1-\varepsilon_0)^2}{\rho g \varepsilon_0^3 \psi^2 d_s^2} - b_1\left(\frac{6(1-\varepsilon_0)}{\psi d_s}\right)^{0.9} v^{0.4}\sigma(t,L) \tag{2.16}$$

with boundary condition $h(t,0) = h_0$, where h_0 is the height of the water layer over the bed.

3. Numerical solution of filtration equations

The filtration model in the form discussed so far is a system of three partial differential equations, the set of initial and boundary conditions, describing functions $C(t,L)$, $\sigma(T,L)$, $h(T,L)$ whose arguments (t,L) are continuous. These equations have analytical solutions only under specific assumptions. In most of the practical cases, however, an analytical solution does not exist and it is thus necessary to solve the differential equations numerically using the finite difference technique. Essentially, the finite difference technique attempts to approximate the continuous solution derived by the exact equations at the discrete points in space (grid points) which overlay the physical domain considered (filter bed) and in time (filter run period), by the so-called difference equations. Difference equations are derived from the differential equations under different approaches.

In this paper, uniform discretization on the rectangular grid, $\Delta t = 10$ min, $\Delta L = 0.5$ cm, was applied with respect to the area shape where the functions discussed are considered. As a result, the functions in question are equivalent to number tables. It is assumed that a row number of a table corresponds to a fixed time, and a column number corresponds to a set bed depth i.e. $t = k\Delta t$, $L = k\Delta L$. In order to obtain a discrete version of the model equations, the simplest, first-order differential approximation of partial derivatives occurring in the equations was applied, resulting in:

$$\frac{C(k,i) - C(k,i-1)}{\Delta L} = -\lambda(\sigma(k,i))C(k,i), \tag{3.1}$$

$$\frac{\sigma(k,i) - \sigma(k-1,i)}{\Delta t} = -v(k-1)\frac{C(k-1,i) - C(k-1,i-1)}{\Delta L}, \tag{3.2}$$

$$\frac{h(k,i) - h(k,i-1)}{\Delta L} = k_1\sigma(k,i) + k_2. \tag{3.3}$$

Alternatively, the second equation may be transformed to the following form:

$$\frac{\sigma(k,i) - \sigma(k-1,i)}{\Delta t} = v(k-1)\lambda(\sigma(k-1,i)).C(k-1,i) \tag{3.4}$$

Solution of the above set of equations with respect to the variables with a "higher" discrete argument yields:

$$C(k,i) = \frac{C(k,i-1)}{1 + \Delta L\lambda(\sigma(k,i))}, \tag{3.5}$$

$$\sigma(k,i) = \sigma(k-1,i) + \Delta t v(k-1)\lambda(\sigma(k-1,i))C(k-1,i), \tag{3.6}$$

$$h(k,i) = h(k,i-1) + \Delta L k_1(\sigma(k,i)) + k_2. \tag{3.7}$$

Due to the above argument, reordering values of variables will be determined for the increasing time and increasing depth in the bed, (see also the diagram presented in Fig. 2). Such order is also consistent with physical nature of the filtration process (17).

The initial and boundary conditions are as follows: $C(k,0)$ – boundary condition (known concentration on the upper bed surface), $\sigma(0,i)$ – initial condition (known concentration of particles accumulated in the bed at the beginning of the process i.e. for $t = 0$), $h(k,0)$ – boundary condition (known pressure on the upper surface of the bed).

The flow diagram for numerical solution of the set (3.5), (3.6), (3.7) is presented in Fig. 2. In this figure rows/columns representing the initial/boundary conditions are marked.

The proposed numerical scheme for solution of model equations is oriented to the case of multilayer filter bed. In such a case each layer can be described by its own set of equations, although in the result of simulations presented later only parameters of equations differ for each layer.

In order to determine the numerical stability of solution with respect to the step of discretization, different values of Δt and ΔL listed in the below tables were examined.

nt	72	144	576
Δt [min]	20	10	2,5

nL	25	50	100	400
ΔL [cm]	8	4	2	0.5

The numerical investigations started with the finest grid (the lowest values of Δt and ΔL, and then the grid squares were enlarged, comparing the obtained graphs of functions $C(t,L)$, $\sigma(t,L)$, $h(t,L)$.

Some examples of the simulation results obtained for the boundary, i.e. the finest and the largest values of the grid squares, are presented in Fig. 3, 4, 5, 6, 8.

It is seen that noticeable differences between the sections of functions $C(t,L)$, $\sigma(t,L)$, $h(t,L)$ for the fixed time periods occur only for function $\sigma(t,L)$ for time t=1h (Fig.) where the graph of the function is discontinuous at point $L = 0.5$m which corresponds to the boundary of the layers.

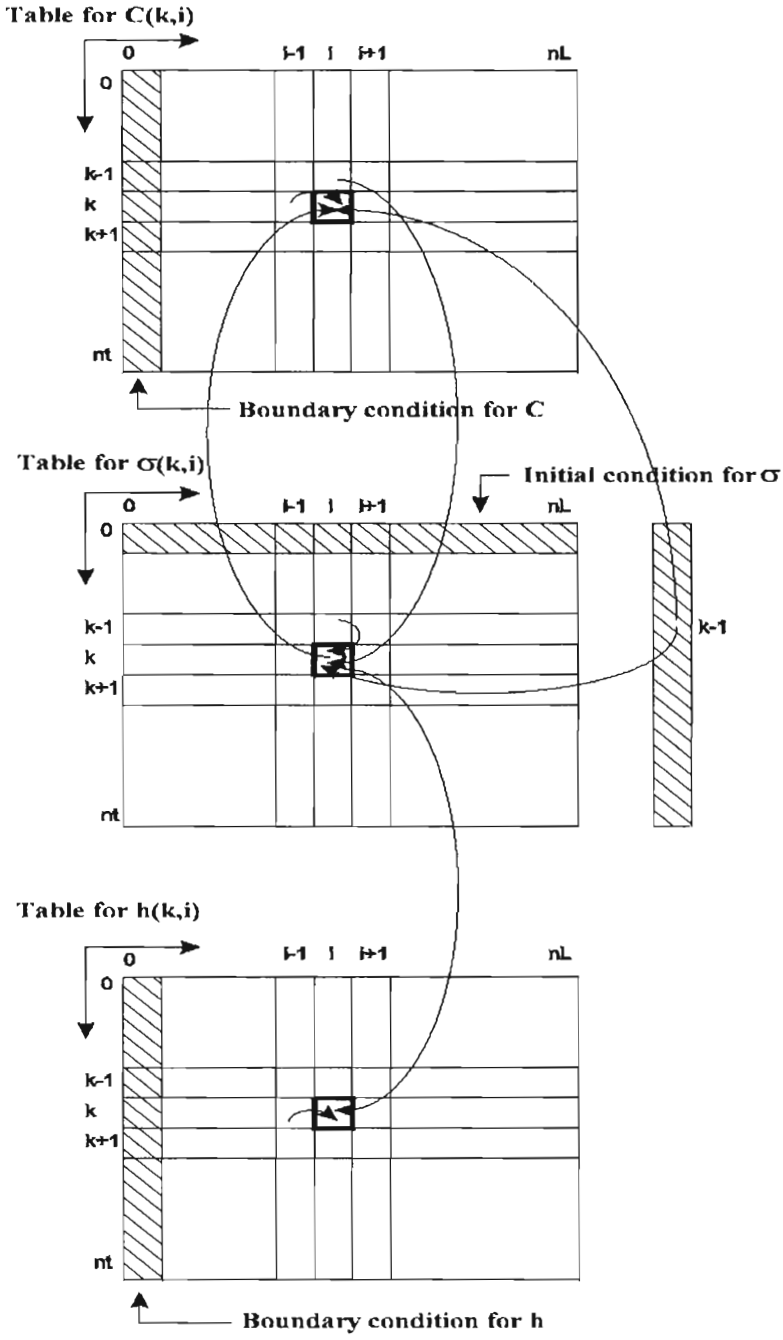

FIG. 2. Flow diagram for tables representing C, σ, h functions and dependences between the elements of the tables which occur in the scheme of numerical solution of model equations.

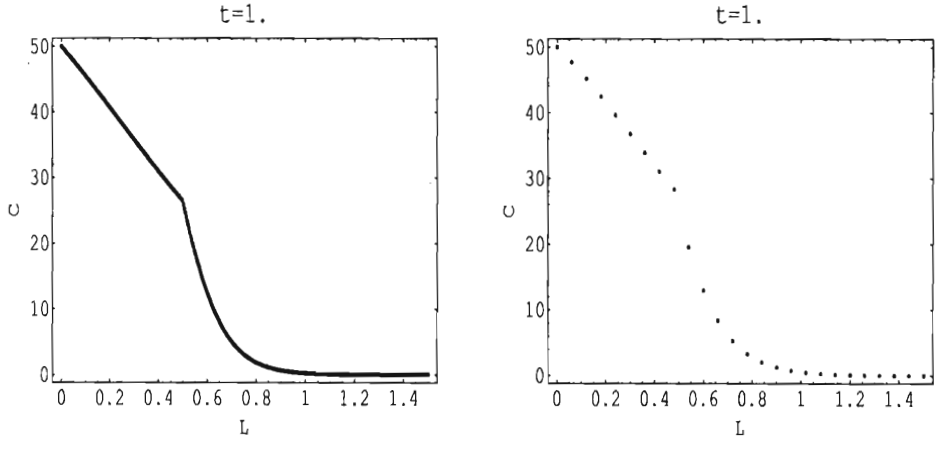

FIG. 3. Mass concentration of particles $C(t, L)[\mathrm{g/m^3}]$ present in the water as a function of depth L[m] in the bed for time instant t=1h and for 576 × 400 and 72 × 25 grid, respectively.

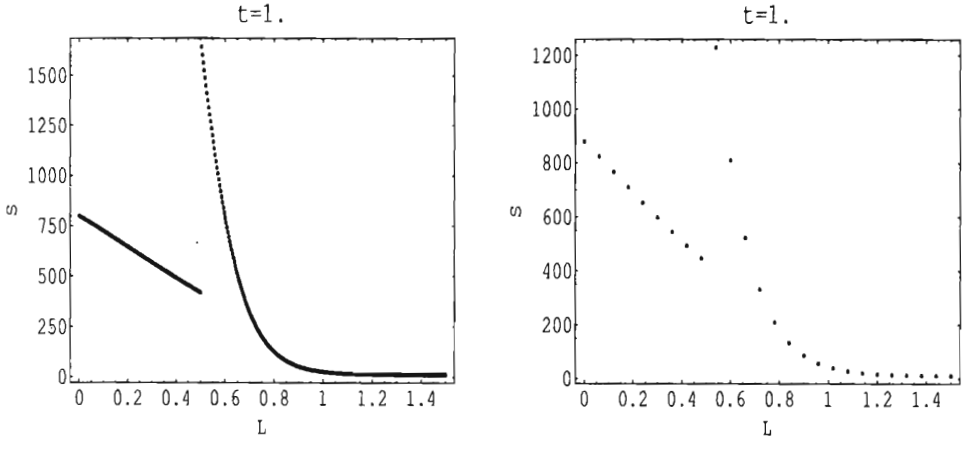

FIG. 4. Mass concentration of particles $\sigma(t, L)[\mathrm{g/m^3}]$ accumulated in the filter bed as a function of depth L[m] in the bed for time instant t=1h and for 576 × 400 and 72 × 25 grid respectively.

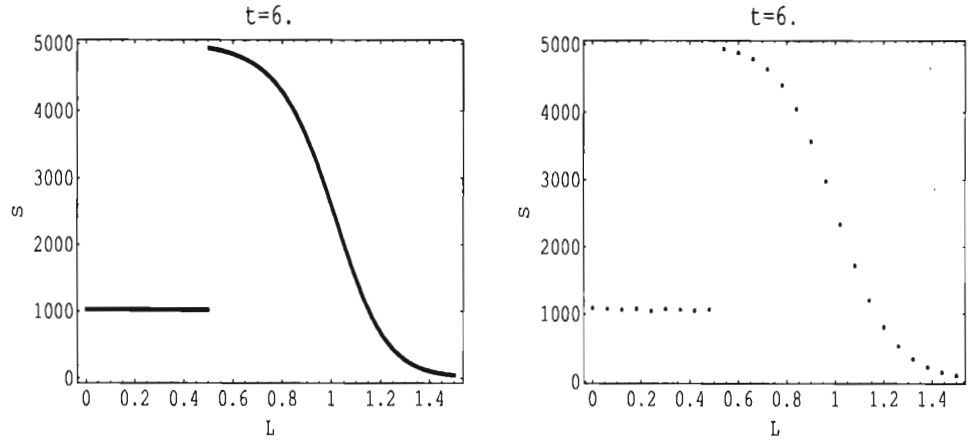

FIG. 5. Mass concentration of particles $\sigma(t, L)[\mathrm{g/m^3}]$ accumulated in the filter bed as a function of depth L[m] in the bed for time instant t=6h and for 576×400 and 72×25 grid respectively.

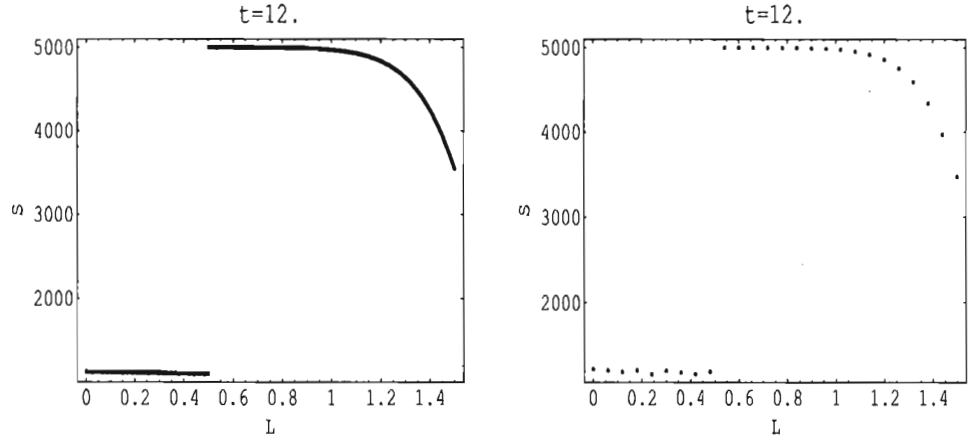

FIG. 6. Mass concentration of particles $\sigma(t, L)[\mathrm{g/m^3}]$ accumulated in the filter bed as a function of depth L[m] in the bed for time instant t=12h and for 576×400 and 72×25 grid respectively.

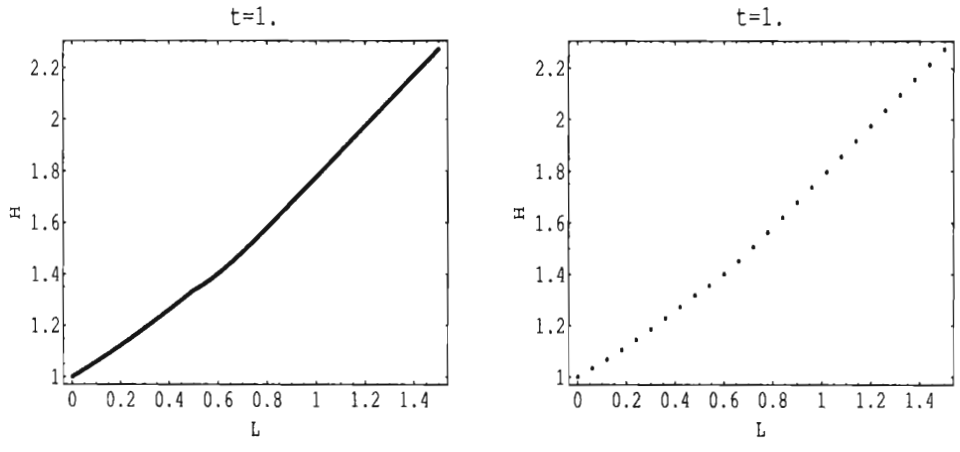

FIG. 7. Pressure $h(t, L)$[m] in the filter bed as a function of depth L[m] in the bed for time instant t=1h and for 576 × 400 and 72 × 25 grid respectively.

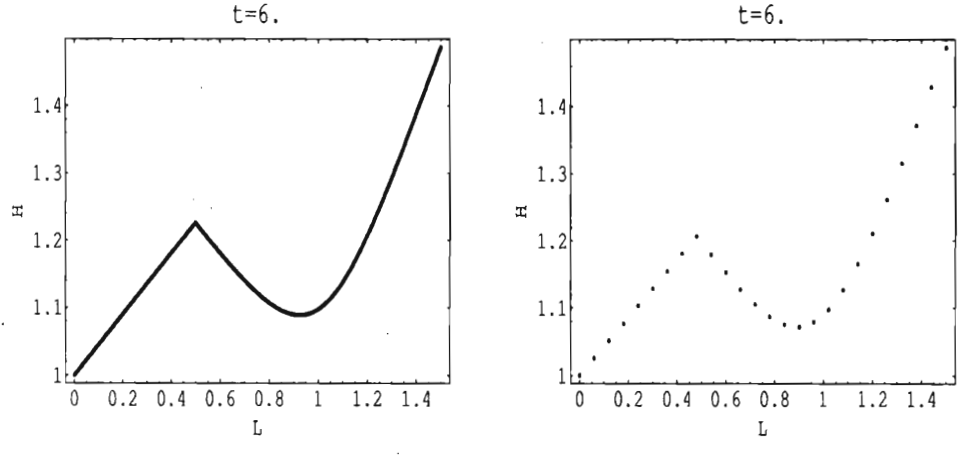

FIG. 8. Pressure $h(t, L)$[m] in the filter bed as a function of depth L[m] in the bed for time instant t=6h and for 576 × 400 and 72 × 25 grid respectively.

The effect of the grid change is more noticeable on 3D graphs, however this results from the rendering technique applied. Some examples which illustrate this effect are presented in Fig. 9.

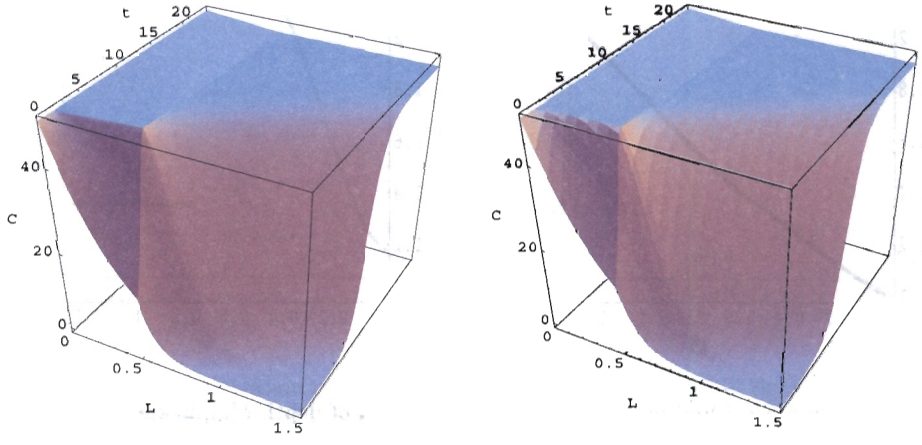

FIG. 9. Mass concentration of particles $C(t, L)[g/m^3]$ present in the water as a function of depth L[m] and time for 576×400 and 72×25 grid respectively.

As a result of the numerical simulations (which results are shown above) carried out to test the stability and accuracy of the suggested method of numerical integration, it has been found that the method is stable and the boundary values of the grid squares are $\Delta L = 4$ cm and $\Delta t = 20$ min. In a case like that, a noticeable difference between the accurate functions $C(t, L)$, $\sigma(t, L)$, $h(t, L)$ and those calculated for grid $\Delta L = 4$ cm and $\Delta t = 20$ min occurs.

Finally, since the graph of function (for the multi-layer beds) is characterized by the step changes on the boundaries of the layers, the relatively low values of $\Delta L = 0.5$ and $\Delta t = 10$ min were assumed.

The discrete model of filtration developed and considered in this chapter may also serve as a basis for identification of parameters and functions present in it. A case when all variables from the model are available for measurements for each point of the grid, and a more complicated case when only some of them are available for some of grid points (e.g. upper and bottom surfaces of the bed) should be noticed here.

4. SIMULATION RESULTS AND ANALYSIS

The numerical simulations were carried out for the exemplary two-layer filtration bed (anthracite, sand) with structure presented in Fig. 10 and under the assumption of fixed level of water during the filtration cycle.

From the point of view of the presented methodology of simulation the increase of number of bed layers is simple.

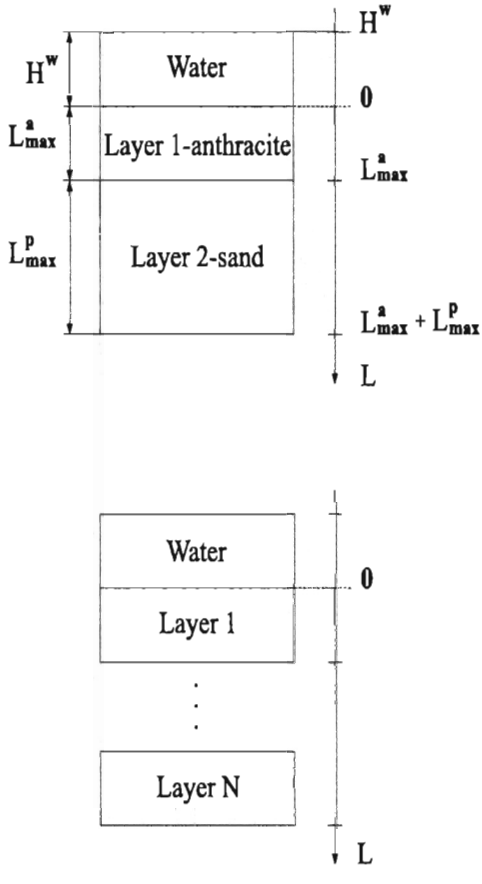

FIG. 10. Exemplary two-layer filter bed (anthracite, sand) and generalized N-layer case

According to the water filtration practice, a suitable 24-hour filtration run (t_{max} = 24h) and a maximum thickness of the bed 2m (L_{max} = 2m) were applied. The simulations discussed hereafter were carried out for the particles concentration in filtered water of 50mg/l, height of water over the bed of 1m, and for constant as well as variable filtration velocity.

Selected simulation results obtained for constant filtration velocity and for two data sets designated with symbols w1 and w2 are shown in figures presented hereafter.

Results of filtration simulation obtained for the exemplary data sets designated as w1 and w2 are presented as graphs of functions $C(t, L)$, $\sigma(t, L)$, $h(t, L)$. This exemplary data sets differ only in filtration velocities, for w1 it is two times

Table 1. Parameters and their numerical values for data sets w1, w2.

PARAMETERS	DATA SETS	
	w1	w2
$H^w = h(t,0)$[m]	1	1
L^a_{max}[m]	0.5	0.5
L^p_{max}[m]	1	1.5
T[h]	24	24
C_0[g/m^3]	50	50
v[m/h]	10	5
ν[m^2/s^{-1}]	$1.5 \cdot 10^{-4}$	$1.5 \cdot 10^{-4}$
d^a_s[mm]	1.4	1.4
d^p_s[mm]	0.75	0.75
ψ^a	0.95	0.95
ψ^p	0.99	0.99
ε^a_0	0.4	0.4
ε^p_0	0.35	0.35
c^a_1	1.145	1.145
c^p_1	2.0	2.0
a^a	0.1	0.1
a^p	0.2	0.2
ρ_s[g/m^3]	$2.4 \cdot 10^6$	$2.4 \cdot 10^6$
ρ^a_s[g/m^3]	$1.65 \cdot 10^6$	$1.65 \cdot 10^6$
ρ^p_s[g/m^3]	$2.65 \cdot 10^6$	$2.65 \cdot 10^6$
c^a_3	$1.2 \cdot 10^{-3}$	$1.2 \cdot 10^{-3}$
c^p_3	$6.3 \cdot 10^{-3}$	$6.3 \cdot 10^{-3}$
c^a_4	0.2	0.2
c^p_4	0.2	0.2
x^a	1.5	1.5
x^p	1.5	1.5
y^a	0.75	0.75
y^p	0.75	0.75
c^a_2	0.45	0.45
c^p_2	0.6	0.6
b^a_1	0.5	0.5
b^p_1	0.8	0.8
K^a_0	0.95	0.95
K^p_0	1.2	1.2
σ^a_u[g/m^3]	10^3	10^3
σ^p_u[g/m^3]	$5 \cdot 10^3$	$5 \cdot 10^3$

higher than for w2 and in thickness of sand layers which are 1m and 1.5m for w1 and w2, respectively.

Analysis of two-dimensional function $C(t, L)$ presented in Fig. 11 and obtained for data set w1 indicates that at the beginning of a filtration run (see one dimensional plot $C(t = 0.6, L)$ Fig. 12), a reduction in particles from 50[mg/l] to 25[mg/l] occurs in the first layer almost linearly with the depth in the layer, and reduction from 25[mg/l] to 0[mg/l] takes place in the second layer of the bed.

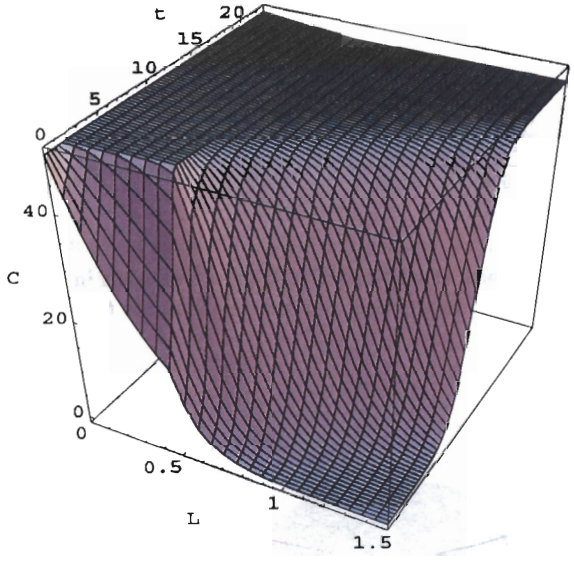

FIG. 11. Mass concentration of particles $C(t, L)$[g/m^3] present in the water as a function of time and depth L[m] in the bed.

The change in particles concentration as a function of depth in the bed is in general an exponential function. Therefore we see that for data set w1, the filtration front reaches the boundary of the layers almost at the beginning of filtration process, thus the concentration of the particles on the boundary is 25[mg/l], and the process of particles deposition in the second layer starts.

Analysis of functions $C(t = const, L)$ for time instants 0.6h, 1.33h Fig. 12 shows that for this stage of a filtration run, a significant decrease in concentration of particles in the filtered water occurs in the first layer. After the capacity of the first layer has reached its limits (see function $C(t = 6, L)$ Fig. 13 and respectively $\sigma(6, L)$ Fig. 17), deposition of particles in the second layer occurs only.

On the basis of the graph of functions $C(t, L)$, $\sigma(t, L)$, presented in Figs. 11, 15 for time instants greater than 10h it can be seen that for data set w1 the time of filtration equal to 24 hours is much longer than practically accepted. Particles concentration at the outlet of the filter exceeded the permissible value.

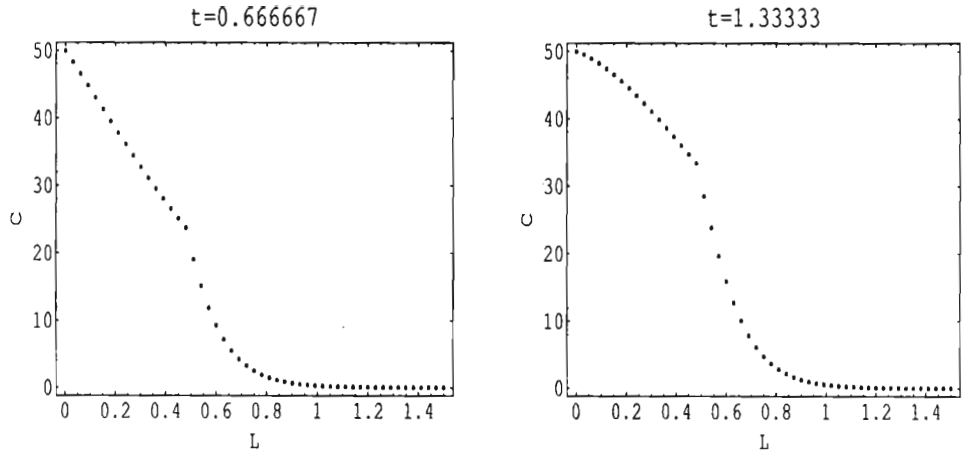

FIG. 12. Mass concentration of particles $C(t, L)[\mathrm{g/m^3}]$ present in the water as a function of depth $L[\mathrm{m}]$ in the bed and for time instants $t = 0.6\mathrm{h};1.3\mathrm{h}$.

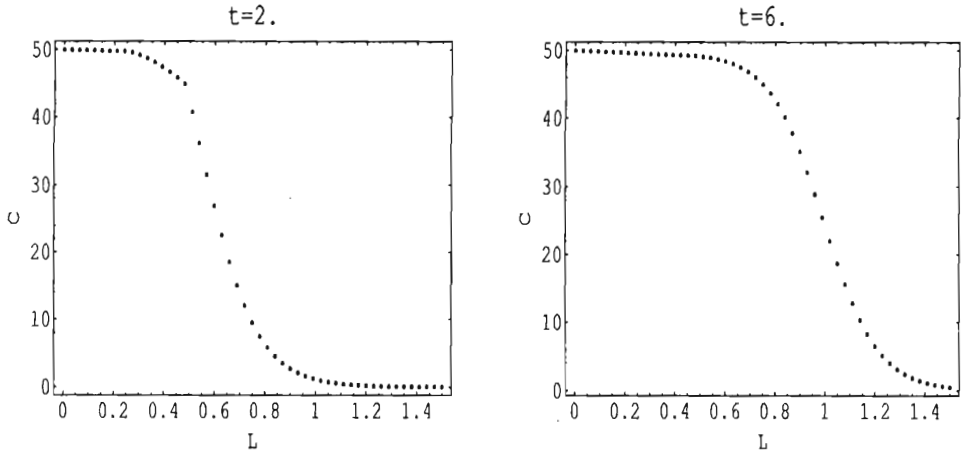

FIG. 13. Mass concentration of particles $C(t, L)[\mathrm{g/m^3}]$ present in the water as a function of depth $L[\mathrm{m}]$ in the bed and for fixed time instants $t = 2\mathrm{h};6\mathrm{h}$.

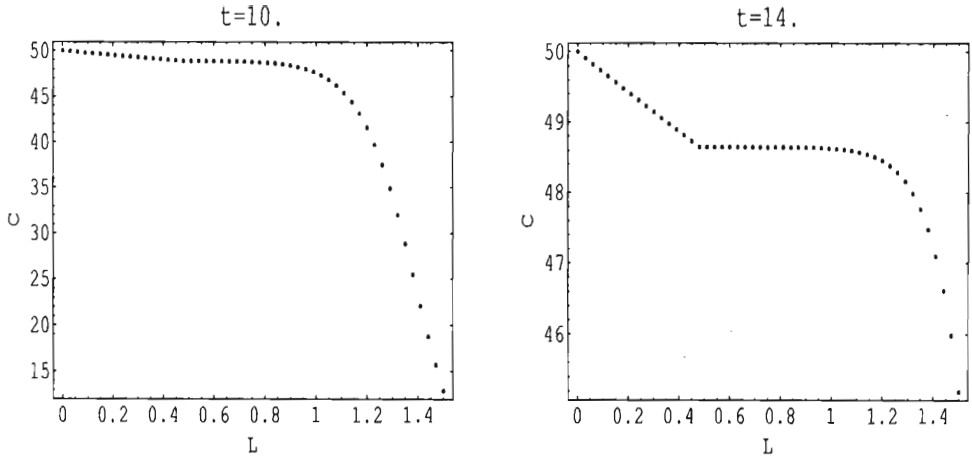

FIG. 14. Mass concentration of particles $C(t, L)[\mathrm{g/m^3}]$ present in the water as a function of depth $L[\mathrm{m}]$ in the bed and for fixed time instants $t = 10\mathrm{h};14\mathrm{h}$.

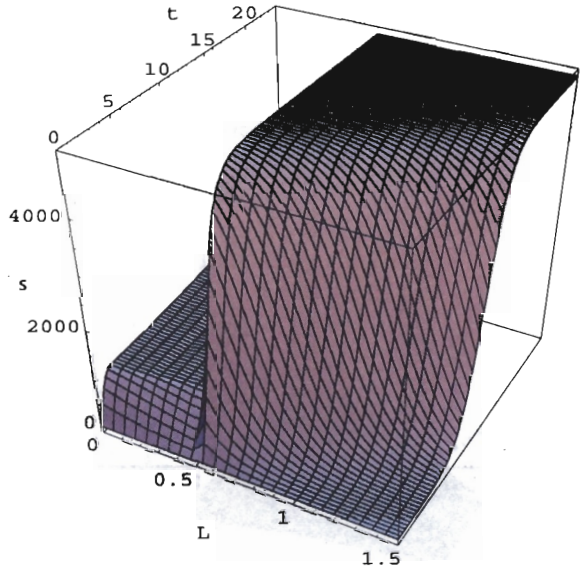

FIG. 15. Mass concentration of particles $\sigma(t, L)[\mathrm{g/m^3}]$ accumulated in the filter as a function of time and depth $L[\mathrm{m}]$ in the bed.

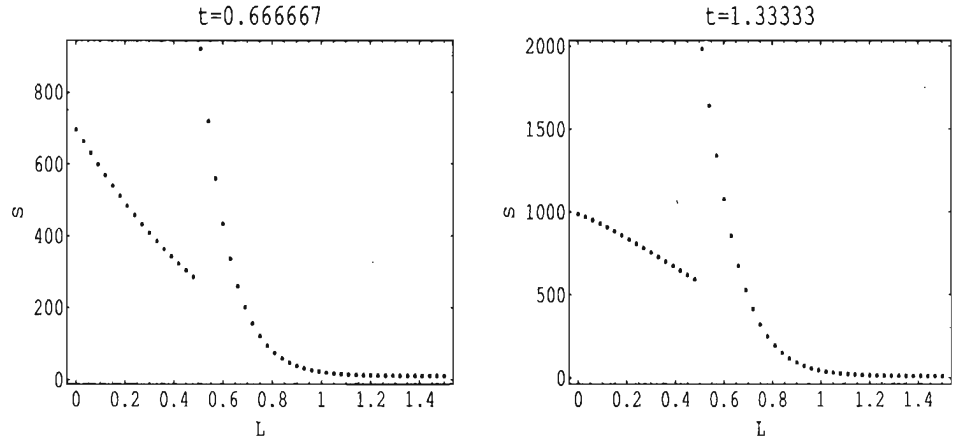

FIG. 16. Mass concentration of particles $\sigma(t, L)[\mathrm{g/m^3}]$ accumulated in the filter as a function of depth L[m] in the bed and for time instants $t = 0.6$h;1.3h.

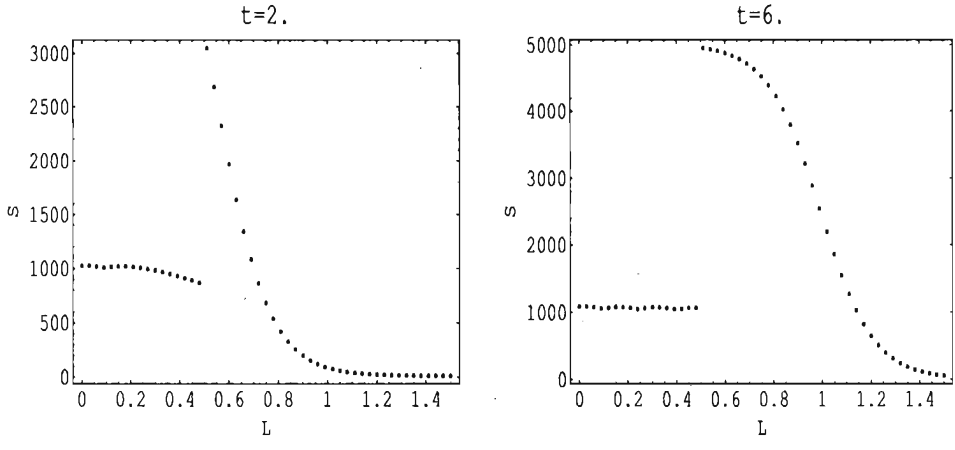

FIG. 17. Mass concentration of particles $\sigma(t, L)[\mathrm{g/m^3}]$ accumulated in the filter as a function of depth L[m] in the bed and for time instants $t = 2$h;6h.

Analysis of function $h(t, L)$ Fig. 19 indicates that it is similar to the one suggested in literature. From the practical point of view, the line of pressures in the bed at the final phase of a filtration run is unsatisfactory due to occurrence of underpressure in a large part of the bed. It should also be noted that because of the five times smaller boundary deposit capacity of the first layer, the head loss from the first layer produced by the particles deposited in this layer is negligible. The head loss that brings about the underpressure occurs in the second layer.

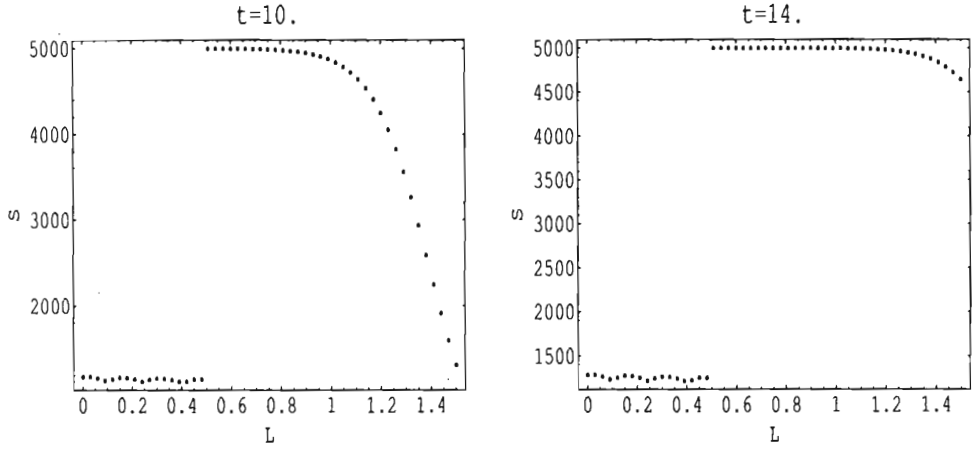

FIG. 18. Mass concentration of particles $\sigma(t, L)[\mathrm{g/m^3}]$ accumulated in the filter as a function of depth $L[\mathrm{m}]$ in the bed and for time instants $t = 10\mathrm{h};14\mathrm{h}$.

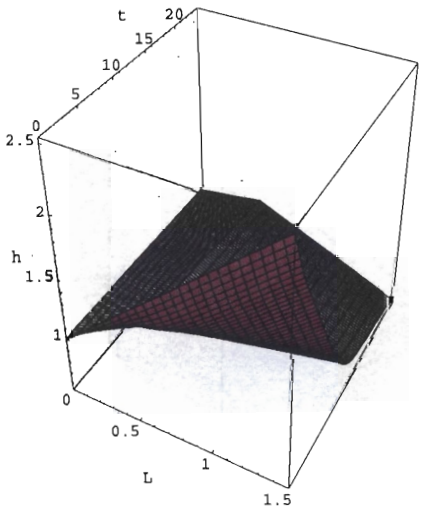

FIG. 19. Pressure $h(t, L)[\mathrm{m}]$ in the filter bed as a function of time and depth $L[\mathrm{m}]$ in the bed.

Analysing qualitatively functions $C(t, L)$, $\sigma(t, L)$, $h(t, L)$, see Figs. 11, 15, 19 it is possible to notice that functions $C(t, L)$, $h(t, L)$ are continuous and function $\sigma(t, L)$ is discontinuous on the boundary of the layers. In other words, there is a step change in the amount of particles deposited in the bed on the boundary of the layers.

In contrast to the above, results of filtration simulation obtained for the exemplary data set w2 which are presented as functions $C(t, L), \sigma(t, L), h(t, L)$ in Figs 23, 24, 25 looks from practical point of view much better. In this case

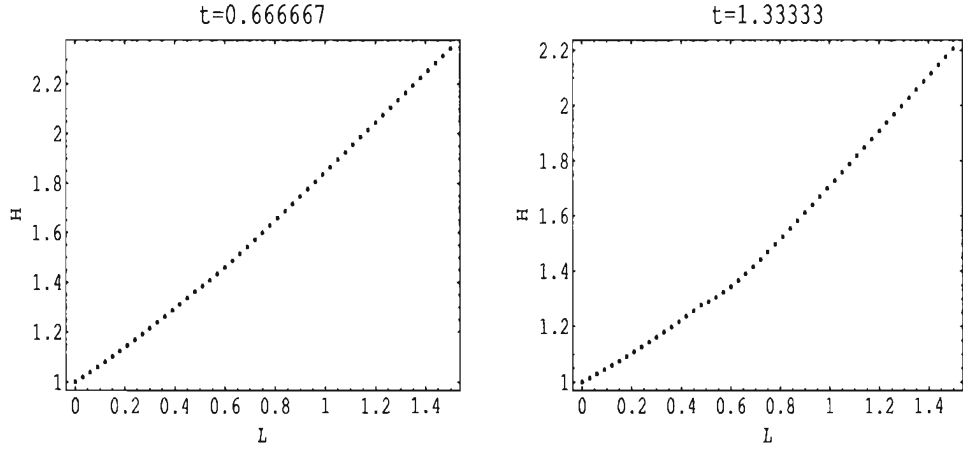

FIG. 20. Pressure $h(t, L)$[m] in the filter bed as a function of depth L[m] in the bed for time instants $t = 0.6$h;1.3h.

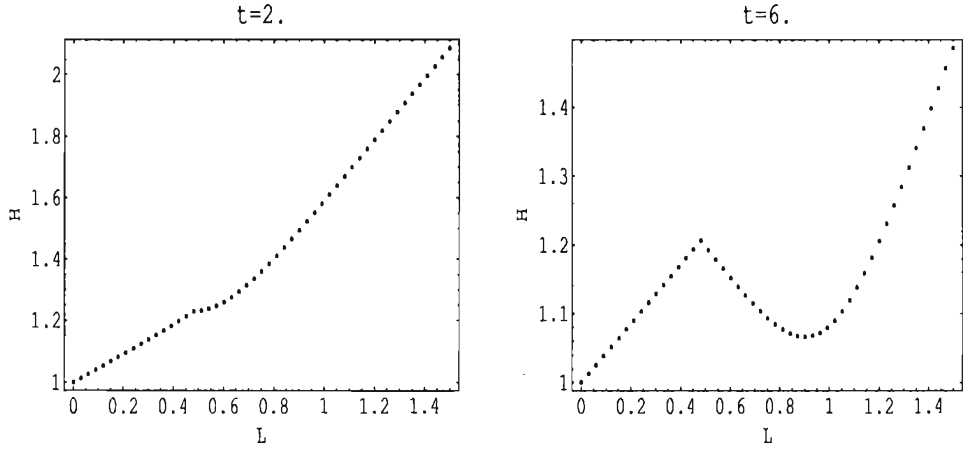

FIG. 21. Pressure $h(t, L)$[m] in the filter bed as a function of depth L[m] in the bed for time instants $t = 2$h;6h.

due to limited space, one-dimensional plots are not included. On the basis of the graphs $C(t,L), \sigma(t,L), h(t,L)$ we can notice, that the simulated filtration time 24 hours is close to maximal. In the w2 data set the filtration velocity is half of that from the w1 data set. Decrease of the filtration velocity means decrease of the particles load brought into the filtration bed. In such a situation, capacity of the bed is sufficient and in the end of the filtration cycle i.e. after 24 hours

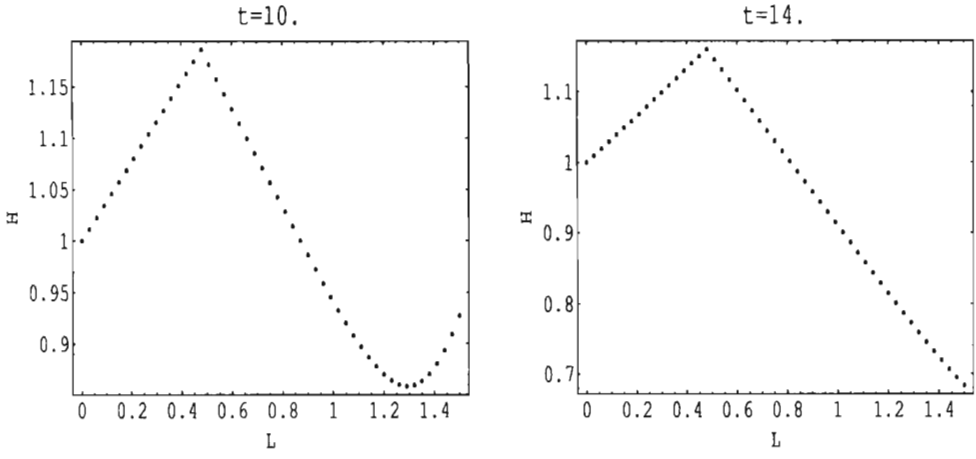

FIG. 22. Pressure $h(t,L)$[m] in the filter bed as a function of depth L[m] in the bed for time instants $t = 10\text{h};14\text{h}$.

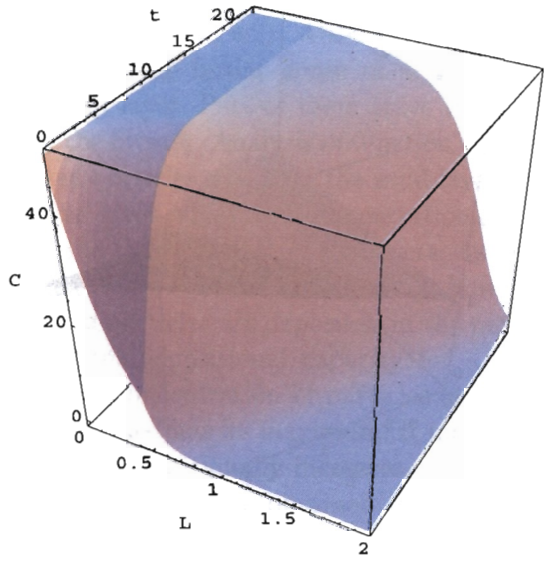

FIG. 23. Mass concentration of particles $C(t,L)[\text{g/m}^3]$ present in the water as a function of time and depth L[m] in the bed for data set w2.

the concentration in the outlet of the filter is still admissible. However, because of nonlinearity due to exponential functions, especially in the first phase of the filtration cycle, possible cycle lengthening is not proportional to the filtration velocity decreasing as well as to the bed layer thickness increasing.

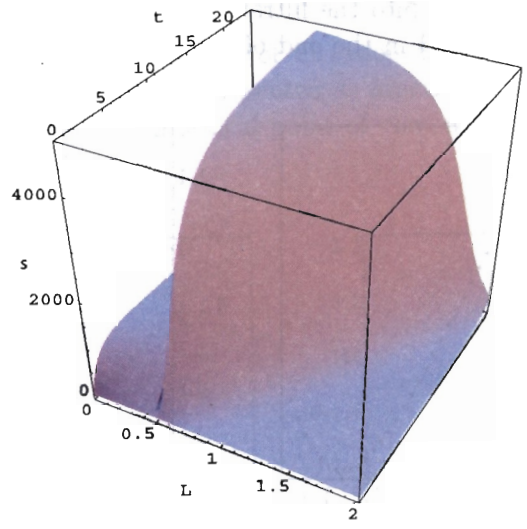

FIG. 24. Mass concentration of particles $\sigma(t, L)$[g/m^3] accumulated in the filter bed as a function of time and depth L [m] in the bed for data set w2.

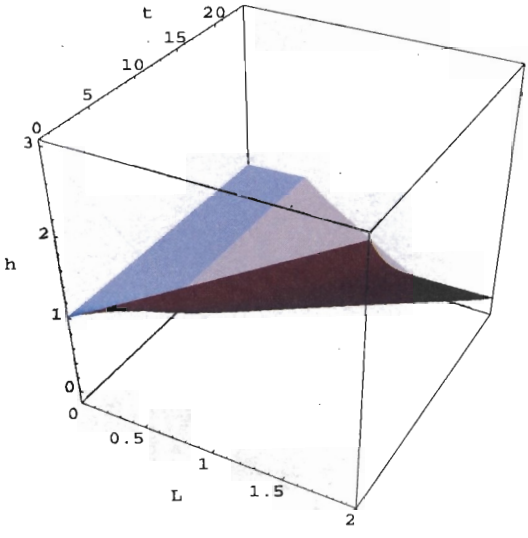

FIG. 25. Presure $h(t, L)$[m] in the filter bed as a function of time and depth L[m] in the bed for data set w2.

Selected results for filtration velocity decreasing and increasing linearly during a filtration run are shown in Figs 26, 27, 29.

Parameters describing the layers are given below where alternative sets of parameters are denoted by symbols w3, w4.

Results of filtration simulation obtained for the data set designated as w3 are presented in Figs. 26, 27, 29 as graphs of functions $C(t, L)$, $\sigma(t, L)$, $h(t, L)$, respectively. In this data set is was assumed that filtration velocity during a filtration run decreases linearly from 5[m/h] to 2[m/h] and the boundary deposit volume of anthracite layer and sand layer are $\sigma_u^a = 10^3$ and $\sigma_u^p = 5 \cdot 10^3$, respectively.

Analysis of function $C(t, L)$ presented in Fig. 26 indicates that at the beginning of a filtration run, a reduction in particles from 50[mg/l] to almost 0[mg/l] takes place in the first layer of the bed. The change in particles concentration as a function of depth L[m] in the bed has a shape of the exponential function. After approximately 1 hour, the filtration front reaches the boundary of the layers and the concentration of the particles on the boundary increases from almost 0 to approximately 15[mg/l], and the process of particles deposition in the second layer starts. Analysis of function $C(t, L)$ shows that in the initial stage of a filtration run, a substantial decrease in concentration of particles in the filtered water occurs in the first layer. After the capacity of the first layer has reached its limits (see cross-section of function $\sigma(t, L)$ presented in Fig. 27 for t=1h), deposition of particles in the second layer starts.

It can be stated that the initial phase of a filtration run from beginning to approximately 7h is qualitatively similar to that for constant filtration velocity (see simulation results for data w1, w2). After the initial phase the particles deposited in the bed during the initial phase of a filtration run are reached and relocated in the second layer. Part of them stays in the filtered water and consequently appears in the filtrate. Analysis of function $C(t, L)$ in Fig. 23 shows that reaching of deposited particles occurs in the sand layer after approximately 7 hours in the part of the layer where the concentration of deposited particles was the highest, i.e. close to the boundary of the layers. As a result, in this area, the concentration of particles in the water increases, however, flowing deeper through the sand layer, the particles are deposited in the part of the layer which did not reach the maximum depositional capacity for a given velocity (filter coefficient is high enough). Concentration of particles considered for a set time as a function of depth in the bed has its maximum. It moves deeper into the bed in the course of filtration and additionally increases.

Exemplifying the simulation results obtained for the filtration velocity increasing with time of a run from 2[mg/l] to 5[mg/l] and presented in Figs 34, 35, 37 indicate that after an initial period of 5 hours, the concentration of particles in the upper layer of the sand bed, similarly to filtration velocity, increases al-

Table 2. Parameters and their numerical values for data sets w3, w4.

PARAMETERS	DATA SETS	
	w3	w4
$H^w = h(t,0)$[m]	1	1
L^a_{max}[m]	0.5	0.5
L^p_{max}[m]	1	1.5
T[h]	24	24
C_0[g/m^3]	50	50
v[m/h]	5 *to* 2	2 *to* 5
ν[m^2/s^{-1}]	$1.5 \cdot 10^{-4}$	$1.5 \cdot 10^{-4}$
d^a_s[mm]	1.4	1.4
d^p_s[mm]	0.75	0.75
ψ^a	0.95	0.95
ψ^p	0.99	0.99
ε^a_0	0.4	0.4
ε^p_0	0.35	0.35
c^a_1	1.145	1.145
c^p_1	2.0	2.0
a^a	0.1	0.1
a^p	0.2	0.2
ρ_s[g/m^3]	$2.4 \cdot 10^6$	$2.4 \cdot 10^6$
ρ^a_s[g/m^3]	$1.65 \cdot 10^6$	$1.65 \cdot 10^6$
ρ^p_s[g/m^3]	$2.65 \cdot 10^6$	$2.65 \cdot 10^6$
c^a_3	$1.2 \cdot 10^{-3}$	$1.2 \cdot 10^{-3}$
c^p_3	$6.3 \cdot 10^{-3}$	$6.3 \cdot 10^{-3}$
c^a_4	0.2	0.2
c^p_4	0.2	0.2
x^a	1.5	1.5
x^p	1.5	1.5
y^a	0.75	0.75
y^p	0.75	0.75
c^a_2	0.45	0.45
c^p_2	0.6	0.6
b^a_1	0.5	0.5
b^p_1	0.8	0.8
K^a_0	0.95	0.95
K^p_0	1.2	1.2
σ^a_u[g/m^3]	10^3	$3 \cdot 10^3$
σ^p_u[g/m^3]	$5 \cdot 10^3$	$5 \cdot 10^3$

most linearly in time; additionally, it reaches a maximum value across the bed depth.

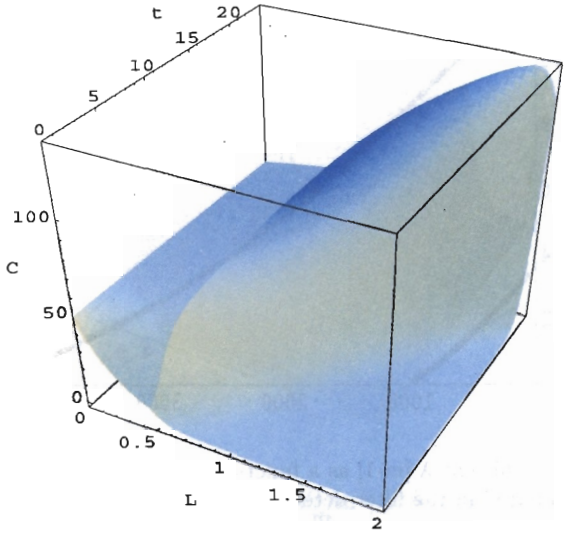

FIG. 26. Mass concentration of particles $C(t, L)[\mathrm{g/m^3}]$ present in the water as a function of time and depth L[m] in the bed determined on the basis of complete model at filtration velocity decreasing linearly over time from $5\frac{m}{h}$ to $2\frac{m}{h}$ and for $w1$ data set.

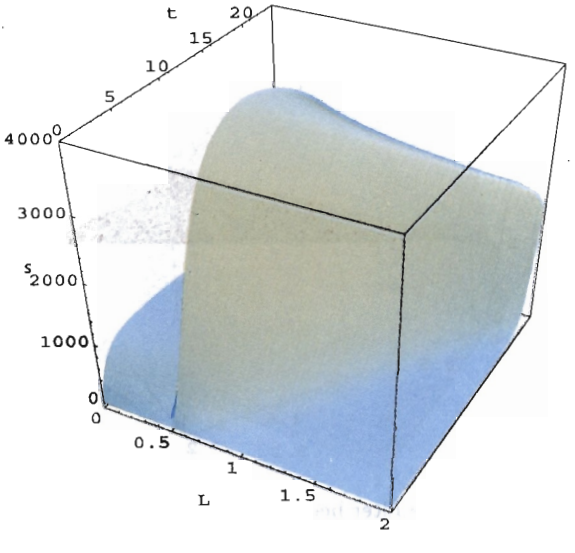

FIG. 27. Mass concentration of particles $\sigma(t, L)[\mathrm{g/m^3}]$ accumulated in the filter as a function of time and depth L[m] in the bed determined on the basis of complete model at filtration velocity decreasing linearly over time from $5\frac{m}{h}$ to $2\frac{m}{h}$ and for $w1$ data set.

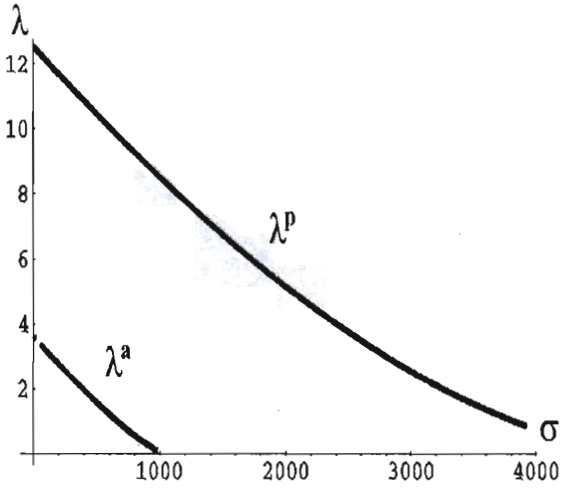

FIG. 28. Filter coefficient λ [m-1] as a function of mass concentration of particles $\sigma(t, L)$[g/m^3] accumulated in the filter determined at filtration velocity decreasing linearly over time from $5\frac{m}{h}$ to $2\frac{m}{h}$ for $w1$ data set.

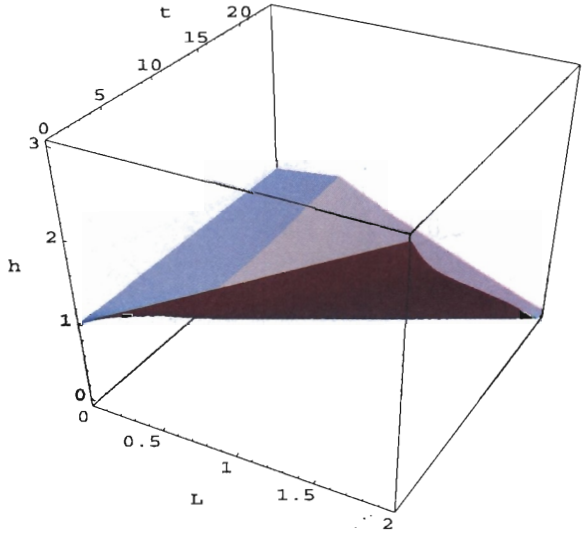

FIG. 29. Pressure $h(t, L)$[m] in the filter bed as a function of time and depth L[m] in the bed determined on the basis of complete model at filtration velocity decreasing linearly over time from $5\frac{m}{h}$ to $2\frac{m}{h}$ for $w1$ data set.

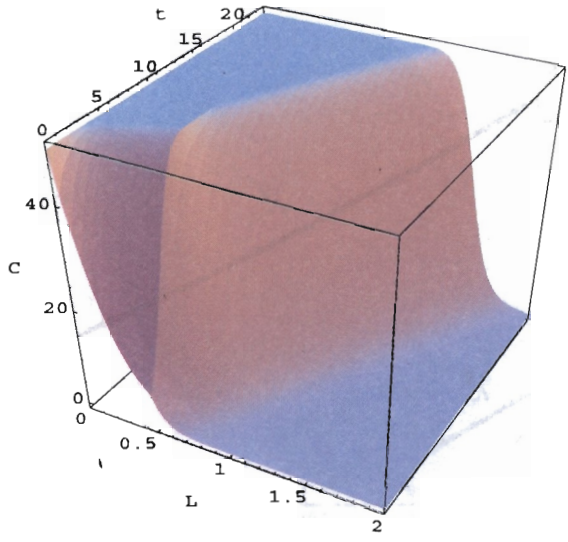

FIG. 30. Mass concentration of particles $C(t, L)[\mathrm{g/m^3}]$ present in the water as a function of time and depth L[m] in the bed determined on the basis of complete model for $w2$ data set.

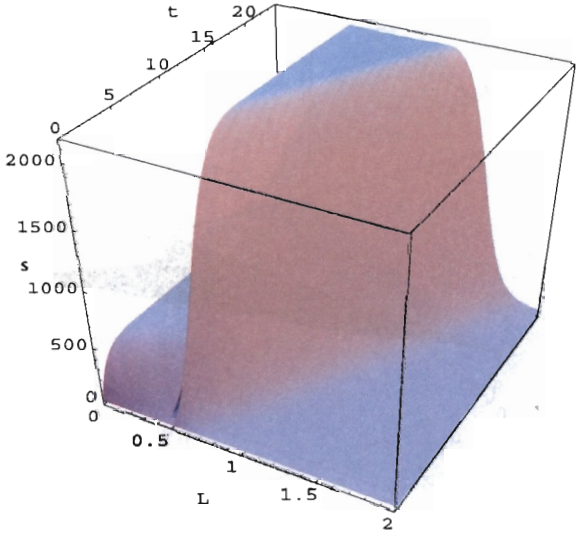

FIG. 31. Mass concentration of particles $\sigma(t, L)[\mathrm{g/m^3}]$ accumulated in the filter as a function of time and depth L[m] in the bed determined on the basis of complete model for $w2$ data set.

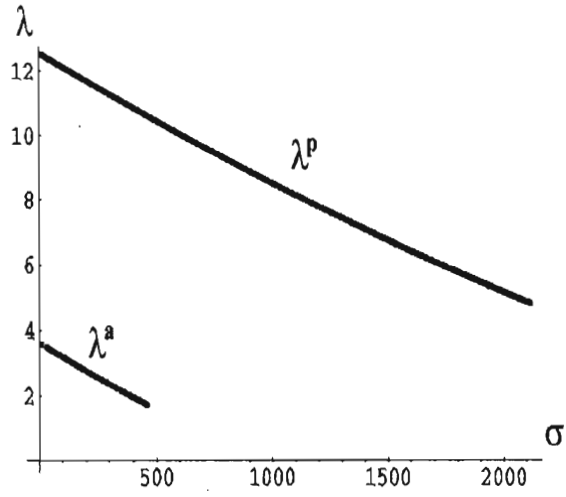

FIG. 32. Filter coefficient $\lambda[\mathrm{m}^{-1}]$ as a function of mass concentration of particles $\sigma(t, L)[\mathrm{g/m}^3]$ accumulated in the filter determined for $w2$ data set.

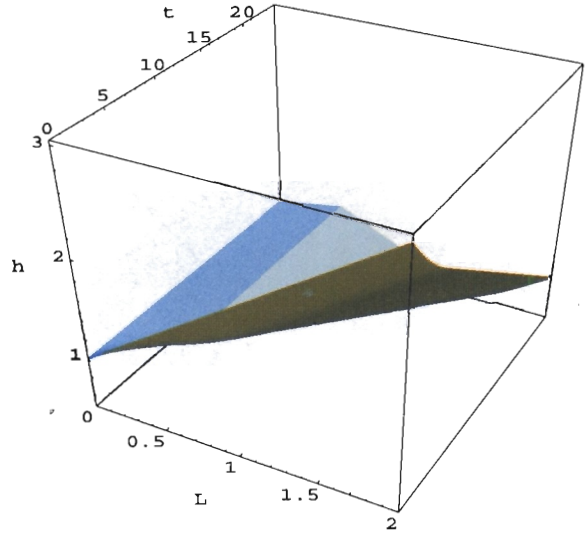

FIG. 33. Pressure $h(t, L)[\mathrm{m}]$ in the filter bed as a function of time and depth $L[\mathrm{m}]$ in the bed determined on the basis of complete model for $w2$ data set.

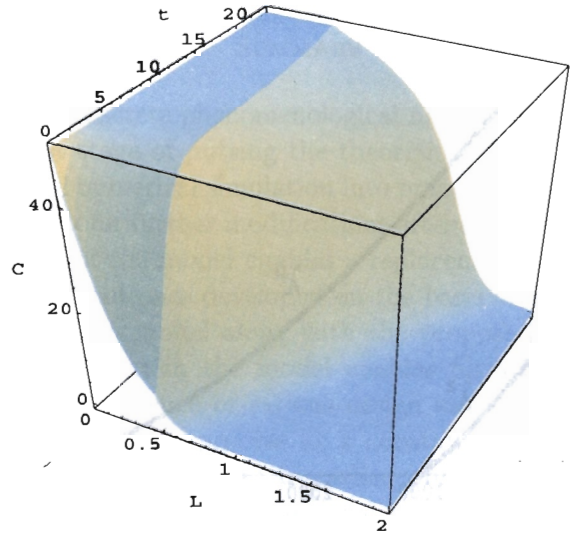

FIG. 34. Mass concentration of particles $C(t, L)[\mathrm{g/m^3}]$ present in the water as a function of time and depth $L[\mathrm{m}]$ in the bed determined on the basis of complete model at filtration velocity increasing linearly over time for $w3$ data set.

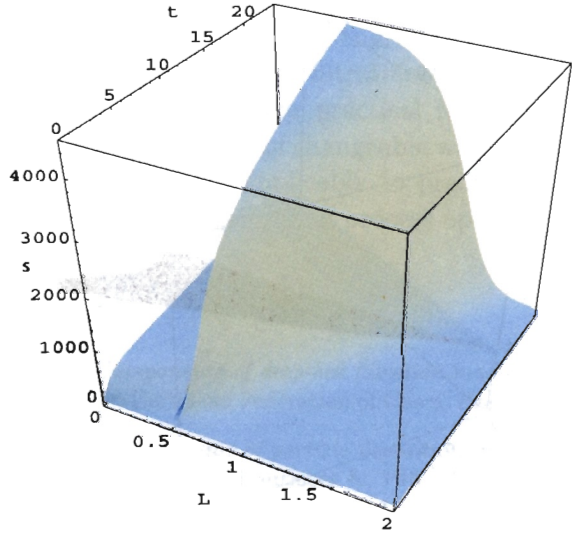

FIG. 35. Mass concentration of particles $\sigma(t, L)[\mathrm{g/m^3}]$ accumulated in the filter as a function of time and depth $L[\mathrm{m}]$ in the bed determined on the basis of complete model at filtration velocity increasing linearly over time for $w3$ data set.

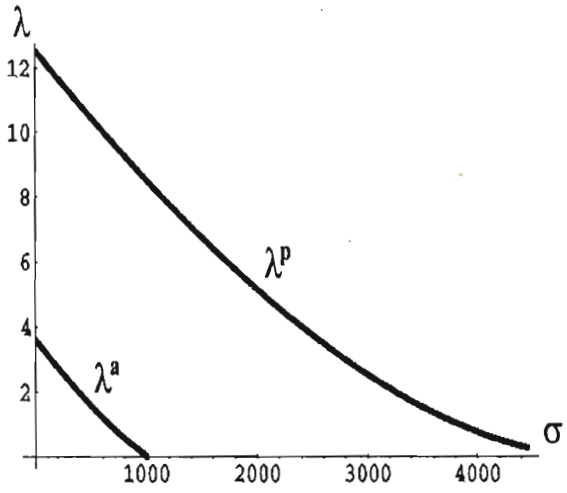

FIG. 36. Filter coefficient $\lambda[\mathrm{m}^{-1}]$ as a function of mass concentration of particles $\sigma(t, L)[\mathrm{g/m}^3]$ accumulated in the filter at filtration velocity increasing linearly over time determined for $w3$ data set.

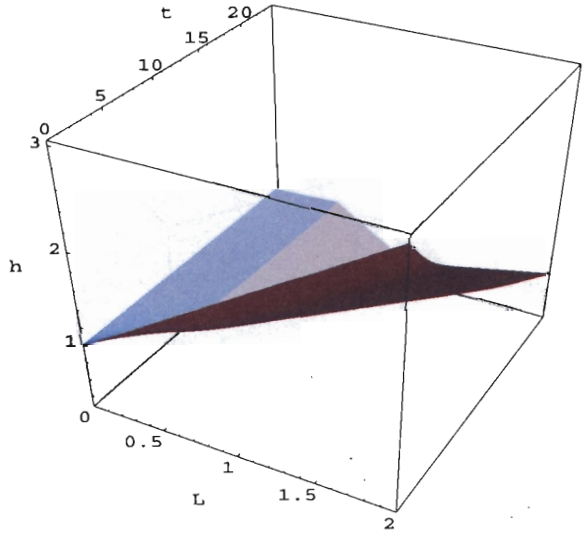

FIG. 37. Pressure $h(t, L)[\mathrm{m}]$ in the filter bed as a function of time and depth $L[\mathrm{m}]$ in the bed determined on the basis of complete model at filtration velocity increasing linearly over time for $w3$ data set.

5. Summary

The continuous and discrete phenomenological filtration models presented in this paper are the first stage of putting the theoretical results obtained during filtration modelling and numerical simulation into practice. The model developed will serve as a framework for further modifications after its numerical verification. The modular structure of the model enables a replacement of selected modules with functionally equivalent ones developed on the basis of different theoretical assumptions. The filtration model along with the proposed numerical method for solving equations present in the model enables filtration simulation, and thus examination of the influence of various design and process parameters on the simulation. Analyses of the process at a constant filtration velocity that followed this approach were presented in earlier works. Simulation results for a two-layer bed showed a qualitative consistency with the values observed in the physical process, confirming the suitability of the model and the numerical methods applied. This consistency between the results of filtration simulation and the phenomena occurring in the course of the real process allows the physical process to be replaced with numerical simulation, as far as design and setting of conditions for operation of rapid filters are concerned. On this basis, a simulation examination of the influence of variable filtration velocity on the course of the process has been attempted. The results obtained in this paper depict interesting phenomena, such as relocation of particles, and contribute to the investigation into the difficult process of non-stationary filtration as far as both the theoretical and practical aspects are concerned. For practical reasons, the non-stationary filtration may be favorable in the cases of changeable water demand. It is believed that the simulation model may be applicable to prediction and simulation of filtration as well as teaching and training of process operators.

References

1. A. Adin, M. Rebhun, *Components of deep-bed filtration mathematical model*, [in:] Proc. Symp. on Water Filtration, European Federation of Chem. Eng., Antwerp, Belgium, 1982.

2. R. Bai, C. Tien, *Transient behavior of particle deposition in granular media under various surface interactions*, Colloids and Surfaces A, **165**, 95-114, 2000.

3. T.P. Camp, *Theory of water filtration*, Journal Sanit. Eng. Div. ASCE, **90**, 1964.

4. J.L. Cleasby, *Water filtration through deep granular media*, Public Works, Junary, 1970.

5. J.L. Cleasby, Di Bernardo, *Hydraulics considerations in declining rate filtration*, Journal Env.Eng.Div., ASCE, EE6, 1980.

6. J.L. Cleasby, *Filtration-back to the basics*, [in:] Proc.AWWA Seminar. Coagulation and Filtration: Back to the Basic, June 1981.

7. H.W. CHANG, C. TIEN, *Dynamics of deep bed filtration*, I.AIChEJ, bf 31, 1349-1360, 1985.

8. C.-U. CHOO, C. TIEN, *Analysis of the transient behaviour of deep bed filtration*, J.Coll.Int.Sci., **169**, 13-33, 1995.

9. J.L. DARBY, D.F. LAWLER, *Ripening in depth filtration: effect of particle size on removal and headloss*, Environ. Sci.Technol., **24**, 1069-1079, 1990.

10. N. FUJISAKI, *An experimental study on dual-media and conventional sand filters*, Journal AWWA, **39**, 1973.

11. K.I. IVES, *The physical and mathematical basic of deep-bed filtration*, Journal Water, **24**, 1937.

12. K.I. IVES, *Mathematical models of deep-bed filtration*, [in:] Scientific Basis of Filtration, Noordhoff International, Leyden 1975.

13. T. IWASAKI, *Some notes on sand filtration*, J.Am.Water Works.Assoc., **29**, 1591-1602, 1937.

14. R.I. MACKIE, R. BAI, *The role of particle size distribution in the performance and modelling of filtration*, Water Sci. Technol., **27**, 19-34, 1993.

15. M.L. MICHELSEN J. VILLDSEN, *A convenient computational procedure of collocation constans*, Chem. Eng. Journal, **4**, 1972.

16. D.M. MINC, W.R. KRISZTNI, *Modielirowanije processa filtracji suspenzyj czerez ziernistyje soi*, Sbornik naucznych rabot AKCh, bf 1, 1960.

17. S.S. MOHANKA, *Theory of multilayer filtration*, Journal of Sanitary Eng. Div., ASCE, **95**, 1969.

18. S.S. MOHANKA, *Multilayer filter design*, Journal Water and Water Engineering, April 1981.

19. C.R. O' MELIA, W. STUMM, *Theory of water filtration*, Journal AWWA, November 1967.

20. C.R. O' MELIA, W. ALI, *The role of retained particles in deep filtration*, Prog. Water Technol., **10**, 167-182, 1978.

21. R.C. RAJAGOPALAN, C. TIEN, *Trajectory analysis of deep-bed filtration with the sphere-in-cell porous media model*, Journal AIChE, **22**, 3, 523, 1976.

22. D.G. STEVENSON, *Flow and filtration through granular media,the effect of grain and particle size dispersion*, Water Res., **31**, 2, 310-322, 1997.

23. C. TIEN, A.C. PAYSTAKES, *Advances in deep-bed filtration*, Journal AIChE, **25**, 737, 1979.

24. C. TIEN, R.M. TURIAN, H. PENDSE, *Simulation of dynamic behaviour of deep bed filters*, Journal AIChE, **25**, 385, 1979.

25. C. TIEN, R. GIMBEL, *On the development of a comprehensive model of deep bed filtration*, [in:] Proc. Sym. on Water Filtration, Belgium, 1982.

26. C. TIEN, *Theoretical analysis of filtration*, [in:] Proc. Int. Tech. Conf. on Filtration and Separation, American Filtration Soc., 1988.

27. J.E. TOBIASSON, G.S. JOHNSON, P.K. WESTERHOFF, *Particle size and filter performance: model studies*, [in:] Nat.Conf.Environ. Eng. Proc. of the 1990 Special Conf., Arlington,VA, 733-739, 1990.

28. S. VIGNESWARAN, J.S. CHANG, J.G. JANSSENS, *Experimental investigation of size distribution of suspended particles in granular bed filtration*, Water Res., **24**, 927-930, 1990.

29. K.M. WOJCIECHOWSKA, *Control of accumulation od solid pollutants in filtration process*, Ochrona Srodowiska [in Polish], **463**, 2-3, 1985.

30. K.M. WOJCIECHOWSKA, *One-dimensional distribution of solids concentration control in a filter bed* [in:], Modeling, Simulation Control, AMSE, **7**, February 1986.

31. K.M. WOJCIECHOWSKA, *Mathematical models of adsorption process for filters designing*, Ochrona Srodowiska [in Polish], **521**, 2-3, 1987.

32. K.M. YAO, M.T. HABIBIAN, C.R. O'MELIA, *Water and wastewater filtration: concepts and applications*, Environ. Sci. Technol., **5**, 1105-1112, 1971.

Received November 11, 2002; revised version February 28, 2002.